

# A New Method to Locate Saddle Points for Reactions in Solution by Using the Free-Energy Gradient Method and the Mean Field Approximation

I. FDEZ. GALVÁN, M. E. MARTÍN, M. A. AGUILAR

Dpto Química Física, Universidad de Extremadura, Avda. de Elvas s/n, 06071, Badajoz, Spain

Received 24 November 2003; Accepted 22 February 2004

DOI 10.1002/jcc.20048

Published online in Wiley InterScience (www.interscience.wiley.com).

**Abstract:** A new method for calculating saddle points of reactions in solution is presented. The main characteristics of the method are: (1) the solute–solvent system is described by the averaged solvent electrostatic potential/molecular dynamics method (ASEP/MD). This is a quantum mechanics/molecular mechanics method (QM/MM) that makes use of the mean field approximation (MFA) and that permits one to simultaneously optimize the electronic structure and geometry of the solute molecule and the solvent structure around it. (2) The transition state is located by the joint use of the free-energy gradient method and the mean field approximation. An application to the study of the Menshutkin reaction between  $\text{NH}_3$  and  $\text{CH}_3\text{Cl}$  in aqueous solution is discussed. The accuracy and usefulness of the proposed method is checked through comparison with other methods.

© 2004 Wiley Periodicals, Inc. J Comput Chem 25: 1227–1233, 2004

**Key words:** solvent effects; Menshutkin reaction; QM/MM; ASEP/MD

## Introduction

The determination of saddle points on free-energy surfaces for a solution reaction is an open question in current computational chemistry. In solution, any successful model must combine an accurate description of the chemical reaction and the solute–solvent interactions. In most cases a full quantum description of the solute–solvent system is impractical or simply unfeasible due to the large number of solvent molecules (several hundred) and configurations (several thousand) that it is necessary to consider to get statistically significant results. Things become even worse if one tries to determine free-energy changes along the reaction path, that is, the potential of mean force. In this case, the number of calculations increases drastically and a full quantum representation, type Car–Parrinello,<sup>1</sup> of the solute–solvent system is impossible except in the simplest cases. For these reasons, in the study of chemical reactions in solution one is compelled to introduce approximations either in the description of the solute or in the description of the solvent.

Two general methods are used in the study of solvent effects. In the first, one simplifies the solvent description, which is implicitly represented through a continuous dielectric medium.<sup>2</sup> In this case, one focuses on the solute molecule that can be described at exactly the same level as is usually employed for *in vacuo* calculations. Examples are the PCM<sup>2a,b</sup> or COSMO<sup>2c,f</sup> methods. The main criticism of these methods is that they neglect the micro-

scopic structure of the solvent around the solute. Furthermore, from a technical point of view it is not clear which are the values of the radii that one must use to construct the solute cavity. The main advantage of continuum models is their low computational cost, similar to *in vacuo* calculations.

In the second, the solvent structure is obtained from simulations. Here, we include Warshel's empirical valence bond (EVB) method<sup>3</sup> and QM/MM methods.<sup>4–6</sup> In both cases one obtains a detailed description of the microscopic structure of the solvent around the solute. EVB represents a reaction in terms of resonance structures and requires a process of parametrization for each chemical reaction. This method permits one to obtain, in an easy way, free energies of molecules and processes in solution. In traditional QM/MM methods one performs a quantum calculation for each solvent configuration generated, so that the number of quantum calculations is greatly increased in this approximation. As a consequence, most calculations to date have been performed at a semiempirical level,<sup>4</sup> although in recent years, and thanks to increasing computational capacity, several models have been proposed where the quantum mechanical calculations are performed at the DFT<sup>5</sup> or HF<sup>6</sup> level.

**Correspondence to:** M. A. Aguilar; e-mail: maguilar@unex.es

Contract/grant sponsor: Consejería de Educación y Juventud de la Junta de Extremadura; contract/grant number: ZPRO3A071

The low computational cost of continuum models comes in part from the introduction of the mean field approximation<sup>7f</sup> (MFA). In this approximation the average of the energies of the different solvent configurations is replaced by the energy of an average configuration. The MFA can also be applied to QM/MM methods. This approximation permits one to greatly reduce the number of quantum calculations, and in consequence, to increase the quality of the quantum description of the solute molecule. To date, two QM/MM methods that make use the MFA have been proposed. The first, known as RISM/SCF, was developed by the Hirata group.<sup>8</sup> Its main characteristic is that the solvent structure is obtained by using an integral theory: the reference interaction site method (RISM). The second, known as ASEP/MD,<sup>7</sup> was developed in our laboratory, and is based on the introduction of the averaged solvent electrostatic potential (ASEP) obtained from molecular dynamics (MD) simulations into the solute molecular Hamiltonian.

In this article we address the problem of the determination of transition states (TS) for reactions in solution. To locate the TS on the free-energy surface (FES) we use a variant<sup>9</sup> of the free-energy gradient method<sup>10</sup> where the derivatives of the free energy are simplified by using the mean field approximation. In this way, both the first and second derivatives of the free-energy surface can be calculated analytically, increasing the computational efficiency of the method.

The proposed method presents several advantages. First, during the ASEP/MD procedure the solute charge distribution and the solvent structure around it become mutually equilibrated. Second, one can use the same (or almost the same) level of quantum mechanical theory as for *in vacuo* calculations, that is, bond-forming and breaking process can be adequately described. Third, once one has determined the solvent structure (through molecular dynamics calculations), the free-energy derivatives are calculated analytically. This greatly increases the ability to explore the free-energy surface and to characterize stationary points. Finally, the model provides detailed information on the solvent structure and on its change during the reaction, so that it is possible to elucidate whether specific solvent molecules influence the reaction mechanism directly.

As an application, in this work we study the Menshutkin reaction (MR)  $\text{NH}_3 + \text{CH}_3\text{Cl} \rightarrow \text{CH}_3\text{NH}_3^+ + \text{Cl}^-$ . From a mechanistic point of view the MR is a special  $\text{S}_\text{N}2$  reaction where the reactants are neutral. Along the reaction coordinate there is a creation of two ions of opposite sign. This process is very unfavorable in the gas phase. In solution, however, the solvent significantly reduces the energy barrier and stabilizes the products. One advantage of this reaction is that it has been studied with RISM/SCF,<sup>8g</sup> QM/MM,<sup>11,12</sup> and continuum<sup>13–15</sup> models, and hence, it is possible to compare the performance of the different methods.

The rest of the article is organized as follows: In the next section the computational method is explained, and especial attention is paid to the definition of the free-energy surface and to the approximations introduced into the calculation of the first and second derivatives of the FES. The results are then discussed, and then we present the main conclusions.

## Method

In this section we describe the extension of the ASEP/MD approach to studying reactions in solution. We begin by defining the nature of the free-energy surface. We estimate the approximate standard free-energy difference between the reactant and transition state in solution as

$$\Delta G_s^0 = \Delta E + \Delta G_{\text{int}} \quad (1)$$

where  $\Delta E$  is the *ab initio* difference between the two QM models (transition state and reactant in our case) and  $\Delta G_{\text{int}}$  is the difference in the solute–solvent interaction free energy. Although formally this equation takes the same form as in the QM-FE approach of Jorgensen et al.<sup>16</sup> the meaning of the  $\Delta E$  term is different, first because the geometries of the transition state and reactant are optimized in solution, and second, because the internal energy and charge distribution of the solute are determined in the presence of the solvent (see below). Obviously, the change in the geometry and charge distribution of the solute also affects the calculation of the  $\Delta G_{\text{int}}$  term.

The saddle-point and minimum structures were located on this approximate free-energy surface,  $G_s^0$ . Once the stationary points on the approximate FES have been obtained, the total activation free-energy changes were calculated by adding the zero-point energy and the entropy and thermal contributions to  $\Delta E$ . It is important to note that these contributions are added *a posteriori* and that, in our case, the vibrational frequencies and molecular geometries necessary for the calculation of the vibrational, rotational, and translational partition functions of the solute were calculated in solution.

The different energies, geometries, vibrational frequencies, and wave functions necessary to calculate  $\Delta G_s^0$  and the zero-point and entropy corrections were obtained by using the ASEP/MD method. This is an iterative procedure that alternates molecular dynamics with quantum mechanics calculations. During the MD simulation the geometry and charge distribution of the solute molecule are considered as fixed. From the MD data we obtain the ASEP that is introduced as a perturbation into the solute molecular Hamiltonian. By solving the associated Schrödinger equation we get a new solute charge distribution and geometry that serves as input for the next MD calculation. The process terminates when convergence in the solute charges, energy, and geometry is reached. The procedure is illustrated in Figure 1.

### Calculation of $\Delta E$

The *ab initio* energy difference between the two QM structures is defined as

$$\Delta E = E_B - E_A = \langle \Psi_B | \hat{H}_B^0 | \Psi_B \rangle - \langle \Psi_A | \hat{H}_A^0 | \Psi_A \rangle \quad (2)$$

Here,  $\hat{H}_X^0$  is the *in vacuo* Hamiltonian of the structure  $X$ , and  $\Psi_X$  is the wave function of the structure  $X$  calculated in the presence of the perturbation due to the solvent.  $\Psi_X$  is obtained by solving the effective Schrödinger equation:

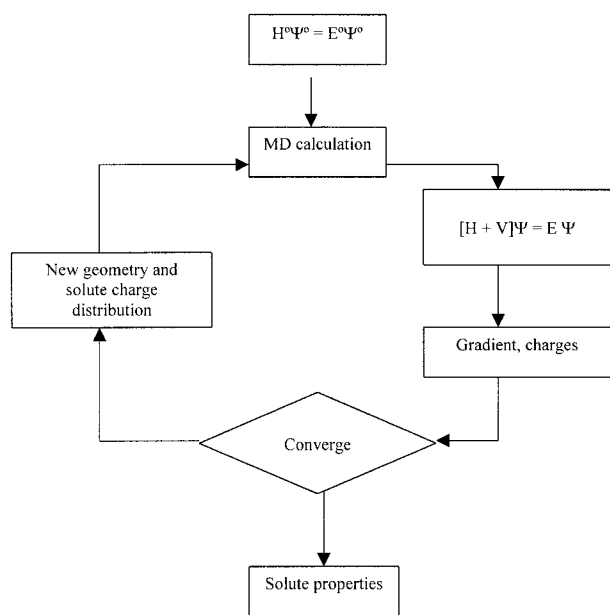


Figure 1. ASEP/MD scheme.

$$(\hat{H}_X^0 + \hat{H}_{\text{QM/MM}})|\Psi\rangle = E|\Psi\rangle \quad (3)$$

The interaction term,  $\hat{H}_{\text{QM/MM}}$ , takes the following form:

$$\hat{H}_{\text{QM/MM}} = \hat{H}_{\text{QM/MM}}^{\text{elect}} + \hat{H}_{\text{QM/MM}}^{\text{vdw}} \quad (4)$$

$$\hat{H}_{\text{QM/MM}}^{\text{elect}} = \int dr \cdot \hat{\rho} \cdot \langle \hat{V}_s(r; \rho) \rangle \quad (5)$$

where  $\hat{\rho}$  is the solute charge density and the brackets denote a statistical average. The term  $\langle \hat{V}_s(r) \rangle$  is the averaged electrostatic potential generated by the solvent at the position  $r$ , and is obtained from MD calculations where the solute molecule is represented by a set of atomic charges and geometry that are kept fixed during the simulation. The term  $\hat{H}_{\text{QM/MM}}^{\text{vdw}}$  is the Hamiltonian for the van der Waals interaction, in general represented by a Lennard–Jones potential. Given that the solvent structure, and hence, the ASEP, is a function of the solute charge density, these two quantities have to be determined iteratively. At each step of the ASEP/MD cycle, the solute charges used in the MD calculation were obtained by fitting the molecular electrostatic potential (MEP) of the solute molecule in the presence of the solvent perturbation. The CHELPG program<sup>17</sup> was used.

In our study, the  $\text{NH}_3$  and  $\text{CH}_3\text{Cl}$  molecules were described using quantum mechanical methods. The rest of the system consisting of the solvent molecules was described through classical mechanics. The basis set used in the description of the quantum part was the aug-cc-pVDZ.<sup>18</sup> The level of calculation was DFT. Following the article of Truong et al.<sup>13</sup> we used a combination of the hybrid Becke's half-and-half functional for exchange and Lee–Yang–Parr functional for correlation (BH&HLYP). From a comparison of several methods those authors conclude that this func-

tional gives the best overall performance. All QM calculations were performed with the Gaussian98<sup>19</sup> suite of programs.

### Calculation of $\Delta G_{\text{int}}$

This magnitude is necessary to calculate the activation free energy but not in the determination of the gradient and Hessians that are calculated directly as the derivatives of the potential energy (see below). In fact,  $\Delta G_{\text{int}}$  is calculated only after the in solution structures of the TS and reactants have been determined.

The free-energy perturbation method was used to determine the free-energy change from the TS to the reactants. The solute geometry was assumed to be rigid and a function of the perturbation parameter ( $\lambda$ ) while the solvent was allowed to move freely.

The contribution of the fluctuations of the QM subsystem to the total free energy, the vibrational entropy of the solute, was calculated with the harmonic contribution. When  $\lambda = 0$ , the solute geometry and charges and the solute–solvent Lennard–Jones parameters correspond to the reactants. When  $\lambda = 1$ , the charges, Lennard–Jones parameters, and geometry are those of the transition state. For intermediate values a linear interpolation is applied. The free-energy difference between the states at  $\lambda$  and  $\lambda + \Delta\lambda$  calculated through free-energy perturbation (FEP) theory is<sup>20,21</sup>

$$\Delta G_\lambda = -RT \ln \left\langle \exp \left( - \frac{\hat{H}_{\text{QM/MM}}(\lambda + \Delta\lambda) - \hat{H}_{\text{QM/MM}}(\lambda)}{RT} \right) \right\rangle_\lambda \quad (6)$$

where  $R$  is the gas constant,  $T$  is the absolute temperature and  $\langle \rangle_\lambda$  denotes the ensemble average at state  $\lambda$ . The total free-energy change between reactants and transition state is thus

$$\Delta G_{\text{int}} = \sum_{\lambda=0}^{\lambda=1} \Delta G_\lambda \quad (7)$$

A value of  $\Delta\lambda = 0.025$  was used. That means that a total of 40 separate molecular dynamics simulations were carried out to determine the free energy. To test the convergence of the calculation, the difference in interaction free energies calculated forward—from the minimum to the saddle point—and backward—from the saddle point to the minimum—are compared. For all the results reported below, the backward and forward activation free energies agree to within less than 5%.

In eq. (6), the solute–solvent interaction energy,  $\hat{H}_{\text{QM/MM}}$ , is calculated classically. This point needs clarification. In the determination of the energies, geometries, and charge distribution of reactants and transition state in solution the solute is quantum mechanically represented. However, once one has determined these magnitudes, the calculation of  $\Delta G_{\text{int}}$  is performed through molecular dynamics simulations where the solute is represented by a set of point charges. In principle, no improvement is expected from replacing the classical by the quantum representation. This is first because the solute charges used in the MD calculation were obtained by fitting the MEP, and hence, they reproduce the QM/MM solute–solvent electrostatic energy, and second, because the free energy is a state function, and hence, its value depends only on the initial and final states (which are quantum mechani-

cally determined) and not on the particular set of charges used in the intermediate steps. For instance, the ASEP/MD method could have been used to obtain the solute charges appropriate for the intermediate geometries. These charges would be different from the ones actually used in the simulations, which are interpolated between the initial and final states. However, as was indicated above, the final energy must be independent of the particular set of charges used in the intermediate steps.

The MD calculations were performed using the program MOLLY.<sup>22</sup> In each case, 214 TIP3P<sup>23</sup> water molecules were simulated at fixed intramolecular geometry. The solute–water potential parameters for the reactants were taken from Carlson et al.<sup>24</sup> (CH<sub>3</sub>Cl) and Ferrario et al.<sup>25</sup> (NH<sub>3</sub>), and the parameters for the TS were taken from Gao and Xia.<sup>11</sup> Periodic boundary conditions, an appropriate cutoff (9.0 Å), and a cubic simulation box of 18.6 Å side were assumed. A time step of 0.5 fs was used. The electrostatic interaction was calculated with the Ewald method. The temperature was fixed at 298 K by using a Nosé–Hoover<sup>26</sup> thermostat. Each MD calculation simulation was run for 150,000 time steps (50,000 equilibration, 100,000 production).

### Quantum Mechanical Determination of Minimum and Saddle Points

In this section we describe the calculation of the gradient and Hessian on the FES. The force on the free-energy surface (FES) is defined as:<sup>10</sup>

$$F(r) = -\frac{\partial G(r)}{\partial r} = -\left\langle \frac{\partial V(r)}{\partial r} \right\rangle \quad (8)$$

where  $G(r)$  is the free-energy,  $V$  is the sum of the contributions associated with the interaction between the atoms of the solute molecule,  $V_i$ , and with the solute–solvent interaction energy,  $V_s$ , and the brackets denote a statistical average.

The Hessian is:

$$H = \left\langle \frac{\partial^2 V}{\partial r \partial r} \right\rangle - \beta \left\langle \frac{\partial V}{\partial r} \frac{\partial V^T}{\partial r} \right\rangle + \beta \left\langle \frac{\partial V}{\partial r} \right\rangle \left\langle \frac{\partial V}{\partial r} \right\rangle^T \quad (9)$$

$$H = \left\langle \frac{\partial^2 V}{\partial r \partial r} \right\rangle - \beta [\langle F^2 \rangle - \beta \langle F \rangle^2] \quad (10)$$

where the superscript  $T$  denotes the transpose and  $\beta = 1/RT$ . The last term in eq. (10) is related to the thermal fluctuation of the force.

At this point we introduce two approximations. First, and following the spirit of the mean field approximation used in ASEP/MD, we replace the average value of the force by the force of the mean configuration:

$$F(r) = -\frac{\partial \langle V \rangle}{\partial r} \quad (11)$$

$$H = \frac{\partial^2 \langle V \rangle}{\partial r \partial r} - \beta \left\langle \frac{\partial V}{\partial r} \frac{\partial V^T}{\partial r} \right\rangle + \beta \frac{\partial \langle V \rangle}{\partial r} \frac{\partial \langle V \rangle}{\partial r}^T \quad (12)$$

Second, we neglect the force fluctuations. With this approximation the Hessian is

$$H = \frac{\partial^2 \langle V \rangle}{\partial r \partial r} \quad (13)$$

Because the stationary points are defined as points where the gradient vanishes, this last approximation has no effect on the geometry of these points. The Hessian is used only to accelerate the search procedure.

The effect of these two approximations has been analyzed in a previous article.<sup>9</sup> We showed that the use of the MFA introduces only small errors into the dipole moment, energies, and gradients. Furthermore, a detailed analysis of the fluctuation term contribution showed that the errors introduced in the trace of the Hessian in the formamide–water systems when we neglected the fluctuation term was less than 5%. A similar error is introduced into the computed frequencies for methanol in the liquid state.

Once the gradient and Hessian are available, the positions of the minimum and saddle point on the FES are determined by the RFO<sup>27</sup> algorithm. It must be stressed that in our method, the solvent is in equilibrium with the charge distribution of the solute at each step of the optimization. As a consequence, nonequilibrium contributions to the activation free energy are completely neglected and, if necessary, must be included *a posteriori*.

## Results and Discussion

To examine the performance of the proposed method we consider the Menshutkin NH<sub>3</sub> + CH<sub>3</sub>Cl reaction in water. The system was partitioned into a QM subsystem (the NH<sub>3</sub> and CH<sub>3</sub>Cl molecules) and an MM system (214 water molecules). The iterative optimization ASEP/MD procedure based on the use of the free-energy gradient method was applied to obtain the optimized structure for the separated reactants and transition state in solution. Then, the activation free-energy change between reactants and TS was determined. In principle, our method yields a true stationary point on the free-energy surface in solution. The computed force constants confirm this.

The Menshutkin reaction has already been studied by different workers using different methods. In the two QM/MM studies<sup>11,12</sup> that have been performed, the solute was represented at the AM1 level. Gao and Xia<sup>11</sup> construct a two-dimensional surface, and the transition state was located on this reduced surface. Hirao et al.<sup>12</sup> locate the TS on a multidimensional free-energy surface obtained by using a variant of the free-energy gradient method proposed by Okuyama–Yoshida et al.<sup>10a</sup> The studies performed with the continuum model, PCM<sup>14,15</sup> and GCOSMO,<sup>13</sup> used different levels of *ab initio* calculations, HF, MCSCF, MP2, MP4, DFT. Truong et al.<sup>13</sup> conclude that, taking as reference the MP4 value, DFT is computationally cheaper and yields more accurate results than MP2 and MCSCF. Consequently, it is our choice in this study. The results of these authors at the DFT level are similar to those obtained by QM/MM methods. Finally, Naka et al.<sup>8g</sup> estimate the free-energy profile by the RISM-MP2 method at the Hartree–Fock optimized geometries along a distinguished reaction coordinate.



**Table 1.** Geometries, Dipole Moments, Atomic Charges, and Solute–Solvent Interaction Energies of the Reactants and Products of the Menshutkin Reaction in the Gas Phase and in Aqueous Solution.

	<i>In vacuo</i>	In solution
CH <sub>3</sub> Cl		
$E_{\text{int}}$	—	−9.36 kcal/mol
C—H	1.086 Å	1.084 Å
C—Cl	1.791 Å	1.798 Å
H—C—Cl	108.1°	107.7°
$q_{\text{C}}$	−0.162 <i>e</i>	−0.106 <i>e</i>
$q_{\text{H}}$	0.115 <i>e</i>	0.118 <i>e</i>
$q_{\text{Cl}}$	−0.183 <i>e</i>	−0.247 <i>e</i>
$\mu$	2.07 D	2.66 D
NH <sub>3</sub>		
$E_{\text{int}}$	—	−15.47 kcal/mol
N—H	1.009 Å	1.012 Å
H—N—H	107.3°	106.3°
$q_{\text{N}}$	−0.898 <i>e</i>	−1.185 <i>e</i>
$q_{\text{H}}$	0.299 <i>e</i>	0.395 <i>e</i>
$\mu$	1.54 D	2.22 D
(NH <sub>3</sub> CH <sub>3</sub> Cl) <sup>‡</sup>		
$E_{\text{int}}$	—	−51.01 kcal/mol
C—H	1.075 Å	1.073 Å
C—N	1.837 Å	2.186 Å
C—Cl	2.443 Å	2.183 Å
N—H	1.010 Å	1.014 Å
Cl—C—H	82.3°	93.8°
C—N—H	110.6°	111.0°
$q_{\text{C}}$	−0.022 <i>e</i>	−0.100 <i>e</i>
$q_{\text{N}}$	−0.361 <i>e</i>	−0.704 <i>e</i>
$q_{\text{Cl}}$	−0.710 <i>e</i>	−0.686 <i>e</i>
$q_{\text{H(C)}}$	0.126 <i>e</i>	0.198 <i>e</i>
$q_{\text{H(N)}}$	0.239 <i>e</i>	0.298 <i>e</i>
$\mu$	12.48 D	11.09 D

Table 1 gives the geometrical parameters, dipole moments, atomic charges, and solute–solvent interaction energies of the reactants and TS in gas phase and in solution. The calculation level used slightly overestimates by +0.18 D the experimental<sup>28</sup> *in vacuo* dipole moment, 1.87 D, of CH<sub>3</sub>Cl. The NH<sub>3</sub> charge distribution is described better. This point is important because in a previous article we showed the importance that a correct description of the solute charge distribution has on the prediction of thermodynamical and structural properties of solutions. Our results slightly improve those obtained by Truong et al.,<sup>13</sup> who use the same functional but a basis set of lower quality.

As shown in Table 1, solvation has an appreciable effect on the polar reactant molecules. The dipole moments of CH<sub>3</sub>Cl and NH<sub>3</sub> increase by 28 and 44%, respectively. In CH<sub>3</sub>Cl, the charge on the hydrogen atoms hardly changes, and the change in the dipole moment is associated to the polarization of the C—Cl bond. For CH<sub>3</sub>Cl, the C—Cl distance increases from 1.791 to 1.798 Å when one passes from vacuum to solution. The solution values are given as the average value of the last five ASEP/MD cycles. The standard deviations are minimal, less than 0.001 Å, 0.1°, and 0.05 D. This indicates that the size of the simulations (75 ps) is adequate: the fluctuations associated with the limited size of the simulation

have a negligible effect on the geometric parameters. The Cl—C—H angle compresses slightly from 108.1° to 107.7°. Similar effects are found for NH<sub>3</sub>: the N—H bond elongates by 0.003 Å and the H—N—H angle is compressed by about 1°.

The solvent effects on the transition state structure are larger: the C—Cl distance decreases from 2.443 to 2.183 Å when one passes from gas phase to solution, and the N—C distance increases from 1.837 to 2.186 Å. In solution, the TS structure is more symmetric, and as a consequence, the dipole moment is lower. The CHelpG charge for the leaving group (Cl) decreases from −0.71 to −0.69 when one passes from vacuum to aqueous solution. Simultaneously, the charge on the N atom increases from −0.36 to −0.70. Given that the charge separation increases along the reaction coordinate, these results indicate that the TS obtained in solution is earlier than the TS in the gas phase, which is in agreement with the Hammond postulate.

As for the free energy of activation, our *in vacuo* result, 44.9 kcal/mol at room temperature, compares very well with the Truong et al.<sup>13</sup> result, 45.7 kcal/mol, as expected from the similar level of calculation. These results are also in good agreement with the AM1 result of Gao and Xia,<sup>11</sup> 46.7 kcal/mol. Solvent effects decrease appreciably the activation free energy. In solution our model yields a value of 25.64 kcal/mol. This value lies between the GCOSMO<sup>13</sup> (24.8 kcal/mol) and AM1/MM values (26.3 kcal/mol if a two-dimensional mapping<sup>11</sup> is used to locate the TS and 26.8–27.1 when the FEG is used<sup>12</sup>). Amovilli et al.<sup>14</sup> using PCM and a 6-311G\*\* basis set obtain 16.8 kcal/mol at the Hartree–Fock level and 20.5 kcal/mol at the CASSCF level. A similar value, 20.9 kcal/mol, is obtained by Naka et al.<sup>8g</sup> with their RISM-MP2 calculation. Experimental data are not available for this system. There is an experimental<sup>29</sup> result (23.5 kcal/mol) for a similar reaction where the CH<sub>3</sub>Cl is replaced by CH<sub>3</sub>I. The differences obtained between the different continuum models, GCOSMO and PCM, are due in part to the level of calculation, but also to the different choice of the cavity radius. In GCOSMO, the atomic radii are adjusted to reproduce free energies of hydration for a representative set of small molecules and ions. In PCM, they are calculated, in general, as 1.2 times the van der Waals radii. Given the great difference that exists between the different versions of the continuum model, a comparison with QM/MM values is complicated. In general, continuum models yield lower activation free energies than QM/MM methods. However, the differences are small and, as has been established in previous articles, we can conclude that in this kind of reaction a nonspecific electrostatic solvent–solute interaction makes the greatest contribution to the TS stabilization.

A direct comparison between our result and other QM/MM results is also complicated by the different level of calculation used (DFT in our case and AM1 in refs. 11 and 12). Furthermore, in the calculation of the activation free energy we include the entropy corrections, which are neglected in the AM1 calculations. However Gao and Xia<sup>11</sup> showed that the AM1 results without entropy corrections provide a reasonable approximation to the *ab initio* free-energy profile obtained at the MP4SDTQ/6-31+G(d) level with scaled frequencies. The same level of calculation (AM1) is used by Hirao et al.<sup>12</sup> If we take the AM1 results as valid, then the agreement between them and our results permits us to conclude that the use of the mean field approximation in the calculation of

**Table 2.** Activation Free Energy (In kcal/mol) and Its Components ( $\Delta V^0$  Stands for the Zero-Point Energy and Thermal Contributions; for the Meaning of the Rest of the Terms, See the Text), and Variation of the Solute–Solvent Interaction Energy from Transition State to Reactants,  $\Delta E_{\text{int}}$ , and Its Electrostatic,  $\Delta E^{\text{elec}}$ , and Lennard–Jones,  $\Delta E^{\text{L-J}}$ , Components.

	<i>In vacuo</i>	In solution
$\Delta E$	32.70	27.48
$\Delta V^0$	12.23	11.86
$\Delta G_{\text{int}}$	—	−13.70
$\Delta G_s^0$ (total)	44.93	25.64
$\Delta E^{\text{elec}}$		−30.50
$\Delta E^{\text{L-J}}$		4.32
$\Delta E_{\text{int}}$		−26.18

gradient and Hessian does not introduce significant errors into the determination of transition states.

Table 2 displays the different contributions to the activation free energy. As one can see, the most important contribution to the decrease of the activation energy when one passes from gas phase to solution comes from the differential solvation free energy. In aqueous solution the TS is better solvated than the reactants. This table also gives the differential solute–solvent interaction energy and its components. As can be seen, the solvent stabilization (−26.18 kcal/mol) is mainly due to the electrostatic (permanent + induced charges) component. In fact, the Lennard–Jones contribution is positive. It stabilizes the reactants in comparison to the TS. The interaction energy does not include the energy spent in polarizing the solvent (in this case, because nonpolarizable molecules are employed for the solvent, it is its structure that is polarized). In classical electrostatics this distortion energy can be obtained as  $-1/2$  of the interaction energy. If the two contributions are added together one obtains the real stabilization produced by the solvent, −13.09 kcal/mol, which agrees very well with the result obtained with the much more computationally demanding free-energy perturbation method, −13.70 kcal/mol.

The evolution of the solvation along the reaction coordinate can be characterized by the changes in the radial distribution functions (rdf), which are shown in Figure 2. The most remarkable fact is the displacement in the position of the first peak of the Cl–O and N–O rdfs from reactants to TS. Simultaneously, the height of the first peak increases, indicating a stronger interaction of the TS with the solvent. Our rdfs compare very well to those obtained by Hirao et al., confirming the validity of the mean field approximation.

## Summary

A new method for determining saddle points in solution has been presented. It is based on the use of the mean field approximation, and permits one to sample the QM/MM potential energy surface properly and to obtain the reaction paths in the solvent environment and the free-energy changes associated with the reactions. The main characteristics of the method are: (1) high-level *ab initio*

quantum calculations are used in the description of the solute molecule; (2) the information about the solvent structure is obtained from MD simulations; (3) the free-energy derivatives are calculated analytically; (4) true stationary points are found, which avoids the definition of a distinguished reaction coordinate. The use of the MFA permits one to greatly reduce the number of quantum calculations and facilitates the calculation of the derivatives. These two points greatly increase the ability of the method to explore the free-energy surface and to find stationary points.

As application of the new method we carried out a study of the Menshutkin reaction  $\text{NH}_3 + \text{CH}_3\text{Cl} \rightarrow \text{CH}_3\text{NH}_3^+ + \text{Cl}^-$  in aqueous solution. In agreement with previous studies we found that the activation energy is greatly reduced by the solvent. In solution, the TS structure is more symmetric than in the gas phase. In agreement with the Hammond postulate, the TS obtained in solution is earlier than the TS in the gas phase.

It was shown, through comparison with the results provided by other methods, that the MFA does not introduce significant errors

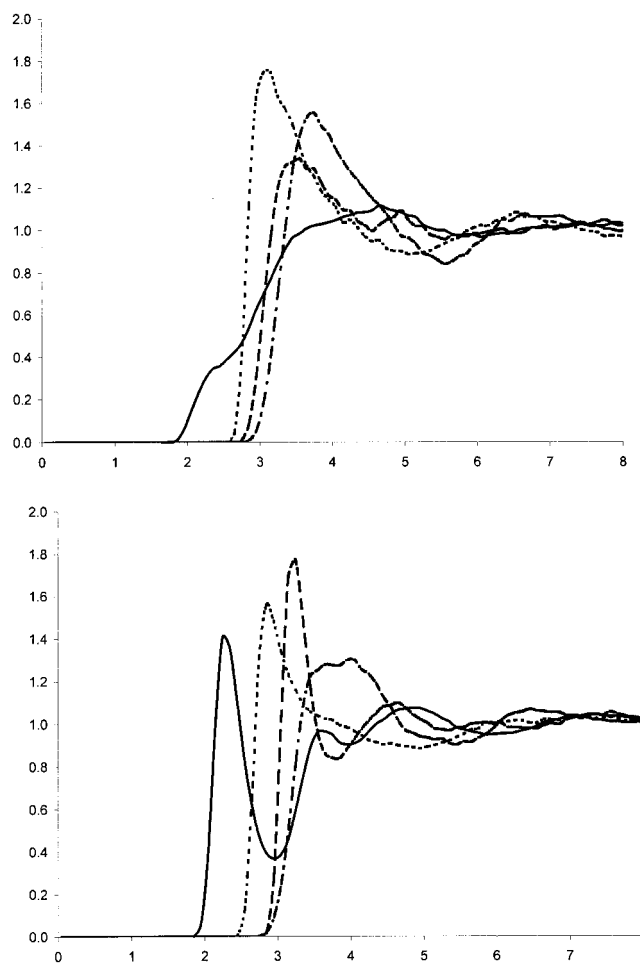


**Figure 2.** Radial distribution functions for reactants (top) and transition state (bottom) of the Menshutkin reaction. Four functions are represented: Cl–H (continuous line), Cl–O (dashed line), N–O (dotted line), and C–O (dash-dotted line).

into either the position of the saddle point or the height of the barrier. We can conclude that the joint use of the ASEP/MD method in the determination of the electronic structure of the solute and the free-energy gradient method and MFA in the determination of the free-energy derivatives constitutes a valid and efficient method for the study of reactions in solution.

## Acknowledgments

The authors acknowledge Dr. José Carlos Corchado for fruitful discussions and help in some calculations.

## References

- Car, R.; Parrinello, M. *Phys Rev Lett* 1985, 55, 2471.
- (a) Tomasi, J.; Bonaccorsi, R.; Cammi, R.; Olivares del Valle, F. J. *J Mol Struct (Theochem)* 1991, 234, 401; (b) Tomasi, J.; Persico, M. *Chem Rev* 1994, 94, 2027; (c) Rivail, J. L.; Rinaldi, D. In *Computational Chemistry: Review of Current Trends*; Leszczynski, J., Ed.; World Scientific Publishing: Singapore, 1995; (d) Cramer, C. J.; Truhlar, D. G. In *Reviews in Computational Chemistry*; Lipkowitz, K. B.; Boyd, D. B., Eds.; VCH Publishers: New York, 1995, p. 1, Vol. VI; (e) Klamt, A.; Schüürmann, J. *Chem Soc Perkin Trans II* 1993, 799; (f) Truong, T. N.; Stefanovich, E. V. *Chem Phys Lett* 1995, 240, 253.
- (a) Warshel, A.; Weiss, R. *J Am Chem Soc* 1980, 102, 6218; (b) Hwang, J.-K.; King, G.; Creighton, S.; Warshel, A. *J Am Chem Soc* 1988, 110, 5297; (c) Åqvist, J.; Warshel, A. *Chem Rev* 1993, 93, 2523.
- (a) Warshel, A.; Levitt, M. *J Mol Biol* 1976, 103, 227; (b) Field, M. J.; Bash, P. A.; Karplus, M. *J Comp Chem* 1990, 11, 700; (c) Luzhkov, V.; Warshel, A. *J Comp Chem* 1992, 13, 199; (d) Gao, J. *J Phys Chem* 1992, 96, 537; (e) Vasilyev, V. V.; Bliznyuk, A. A.; Voityuk, A. A. *Int J Quantum Chem* 1992, 44, 897; (f) Théry, V.; Rinaldi, D.; Rivail, J.-L.; Maignet, B.; Ferenczy, G. G. *J Comp Chem* 1994, 15, 269; (g) Thompson, M. A.; Glendening, E. D.; Feller, D. *J Phys Chem* 1994, 98, 10465.
- (a) Wei, D.; Salahub, D. R. *Chem Phys Lett* 1994, 224, 291; (b) Tuñón, I.; Martins-Costa, M. T. C.; Millot, C.; Ruiz-López, M. F.; Rivail, J.-L. *J Comp Chem* 1996, 17, 19; (c) Wesolowski, T. A.; Warshel, A. *J Phys Chem* 1993, 97, 8050; *J Phys Chem* 1994, 98, 5183; (d) Wesolowski, T. A.; Muller, R. P.; Warshel, A. *J Phys Chem* 1996, 100, 15444.
- (a) Vaidehi, N.; Wesolowski, T. A.; Warshel, A. *J Chem Phys* 1992, 97, 4264; (b) Stanton, R. V.; Little, L. R.; Merz, K. M. *J Phys Chem* 1995, 99, 17344; (c) Moriarty, N. W.; Karlström, G. *J Phys Chem* 1996, 100, 17791; (d) Tu, Y.; Laaksonen, A. *J Chem Phys* 1999, 111, 7519.
- (a) Sánchez, M. L.; Aguilar, M. A.; Olivares del Valle, F. J. *J Comp Chem* 1997, 18, 313; (b) Sánchez, M. L.; Martín, M. E.; Aguilar, M. A.; Olivares del Valle, F. J. *Chem Phys Lett* 1999, 310, 1995; (c) Sánchez, M. L.; Martín, M. E.; Aguilar, M. A.; Olivares del Valle, F. J. *J Comp Chem* 2000, 21, 705; (d) Martín, M. E.; Sánchez, M. L.; Olivares del Valle, F. J.; Aguilar, M. A. *J Chem Phys* 2000, 113, 6308; (e) Muñoz Losa, A.; Fdez. Galván, I.; Martín, M. E.; Aguilar, M. A. *J Phys Chem B* 2003, 107, 5043; (f) Sánchez, M. L.; Martín, M. E.; Fdez. Galván, I.; Olivares del Valle, F. J.; Aguilar, M. A. *J Phys Chem B* 2002, 106, 4813.
- (a) Ten-no, S.; Hirata, F.; Kato, S. *Chem Phys Lett* 1993, 214, 391; (b) Ten-no, S.; Hirata, F.; Kato, S. *J Chem Phys* 1994, 100, 7443; (c) Kawata, M.; Ten-no, S.; Kato, S.; Hirata, F. *Chem Phys* 1995, 240, 199; (d) Kawata, M.; Ten-no, S.; Kato, S.; Hirata, F. *J Phys Chem* 1996, 100, 1111; (e) Kinoshita, M.; Okamoto, Y.; Hirata, F. *J Comp Chem* 1997, 18, 1320; (f) Akiyama, R.; Hirata, F. *J Chem Phys* 1998, 108, 4904; (g) Sato, H.; Kovalenko, A.; Hirata, F. *J Chem Phys* 2000, 112, 9463; (h) Naka, K.; Sato, H.; Morita, A.; Hirata, F.; Kato, S. *Theor Chem Acc* 1999, 102, 165.
- Fdez. Galván, I.; Sánchez, M. L.; Martín, M. E.; Olivares del Valle, F. J.; Aguilar, M. A. *J Chem Phys* 2003, 118, 255.
- (a) Okuyama-Yoshida, N.; Nagaoka, M.; Yamabe, T. *Int J Quantum Chem* 1998, 70, 95; (b) Okuyama-Yoshida, N.; Kataoka, K.; Nagaoka, M.; Yamabe, T. *J Chem Phys* 2000, 113, 3519.
- Gao, J.; Xia, X. *J Am Chem Soc* 1993, 115, 9667.
- Hirao, H.; Nagae, Y.; Nagaoka, M. *Chem Phys Lett* 2001, 348, 350.
- Truong, T. N.; Truong, T.-T. T.; Stefanovich, E. V. *J Chem Phys* 1997, 107, 1881.
- Amovilli, C. A.; Mennucci, B.; Floris, F. M. *J Phys Chem B* 1998, 102, 3023.
- Fradera, X.; Amat, L.; Torrent, M.; Mestres, J.; Constans, P.; Besalú, E.; Martí, J.; Simon, S.; Lobato, M.; Oliva, J. M.; Luis, J. M.; Andrés, J. L.; Solà, M.; Carbó, R.; Duran, M. *J Mol Struct (Theochem)* 1996, 371, 171.
- (a) Chandrasekhar, J.; Smith, S. F.; Jorgensen, W. L. *J Am Chem Soc* 1985, 107, 154; (b) Chandrasekhar, J.; Jorgensen, W. L. *J Am Chem Soc* 1985, 107, 2974; (c) Jorgensen, W. L. *Acc Chem Res* 1989, 22, 184.
- (a) Chirlian, L. E.; Francl, M. M. *J Comp Chem* 1987, 8, 894; (b) Breneman, C. M.; Wiberg, K. B. *J Comp Chem* 1990, 11, 316.
- (a) Dunning, T. H., Jr. *J Chem Phys* 1989, 90, 1007; (b) Kendall, R. A.; Dunning, T. H., Jr.; Harrison, R. J. *J Chem Phys* 1992, 96, 6796; (c) Woon, D. E.; Dunning, T. H., Jr. *J Chem Phys* 1993, 98, 1358.
- Frisch, M. J.; Trucks, G. W.; Schlegel, H. B.; Scuseria, G. E.; Robb, M. A.; Cheeseman, J. R.; Zakrzewski, V. G.; Montgomery, J. A., Jr.; Stratmann, R. E.; Burant, J. C.; Dapprich, S.; Millam, J. M.; Daniels, A. D.; Kudin, K. N.; Strain, M. C.; Farkas, O.; Tomasi, J.; Barone, V.; Cossi, M.; Cammi, R.; Mennucci, B.; Pomelli, C.; Adamo, C.; Clifford, S.; Ochterski, J.; Petersson, G. A.; Ayala, P. Y.; Cui, Q.; Morokuma, K.; Malick, D. K.; Rabuck, A. D.; Raghavachari, K.; Foresman, J. B.; Cioslowski, J.; Ortiz, J. V.; Baboul, A. G.; Stefanov, B. B.; Liu, G.; Liashenko, A.; Piskorz, P.; Komaromi, I.; Gomperts, R.; Martin, R. L.; Fox, D. J.; Keith, T.; Al-Laham, M. A.; Peng, C. Y.; Nanayakkara, A.; Gonzalez, C.; Challacombe, M.; Gill, P. M. W.; Johnson, B.; Chen, W.; Wong, M. W.; Andres, J. L.; Gonzalez, C.; Head-Gordon, M.; Replogle, E. S.; Pople, J. A. *Gaussian 98*; Gaussian, Inc.: Pittsburgh, PA, 1998.
- Kollman, P. A. *Chem Rev* 1993, 93, 2395.
- Mark, A. E. In *Encyclopedia of Computational Chemistry*, Schleyer, P. V. R.; Allinger, N. L.; Clark, T.; Gasteiger, J.; Kollman, P. A.; Schaefer, H. F., III; Schreiner, P. R., Eds.; Wiley and Sons: Chichester, 1998, p. 1070, Vol. 2.
- Refson, K. *Comp Phys Commun* 2000, 126, 310.
- Jorgensen, W. L.; Chandrasekhar, J.; Madura, J. D.; Impey, R. W.; Klein, M. L. *J Chem Phys* 1983, 79, 926.
- Carlson, H. A.; Nguyen, T. B.; Orozco, M.; Jorgensen, W. L. *J Comp Chem* 1993, 14, 1240.
- Ferrario, M.; Haughney, M.; McDonald, I. R.; Klein, M. L. *J Chem Phys* 1990, 93, 5156.
- Hoover, W. G. *Phys Rev A* 1985, 31, 1695.
- (a) Simons, J.; Jørgensen, P.; Taylor, H.; Ozment, J. *J Phys Chem* 1983, 87, 2745; (b) Banerjee, A.; Adams, N.; Simons, J.; Shepard, R. *J Phys Chem* 1985, 89, 82; (c) Baker, J. *J Comp Chem* 1986, 7, 385.
- de Jongh, J. P.; Dijkerman, H. A. *J Mol Spectrosc* 1968, 25, 129.
- Okamoto, K.; Fukui, S.; Shingu, H. *Bull Chem Soc Jpn* 1967, 40, 1920.